Desalination and Water Treatment
www.deswater.com

doi: 10.5004/dwt.2020.25018

179 (2020) 38–44
March

Synergistic effect of ATMP, EDTMPS and PESA on the scale inhibition in the reinjected sewage

Jiajia Wang[a,b], Guojun Shi[b,*], Hongbing Zhu[c]

[a]*Guangling College, Yangzhou University, Yangzhou 225000, Jiangsu Province, China, email: wangjiajia20170801@163.com*
[b]*School of Chemistry and Chemical Engineering, Yangzhou University, Yangzhou 225002, Jiangsu Province, China, Tel./Fax: +86-514-87937661; email: gjshi@yzu.edu.cn*
[c]*Yangzhou Runda Oilfield Chemicals Co. Ltd., Yangzhou 225261, Jiangsu Province, China, email: 2467166751@qq.com*

Received 21 December 2018; Accepted 13 October 2019

ABSTRACT

The amino trimethylene phosphonic acid (ATMP), ethylene diamine tetra (methylene phosphonic acid) sodium (EDTMPS) and polyepoxysuccinic acid (PESA) were used as the starting materials to prepare the blend antiscalants against the formations of $CaSO_4{\cdot}2H_2O$ scales. A remarkable synergistic effect was observed between ATMP and PESA at an arbitrary proportion, and PESA and EDTMPS showed an optimal synergistic effect at a PESA/EDTMPS mass ratio of 5:1. The observed inhibiting roles of the blended binary antiscalants were much better than that of the individual ones. The blends A_2P (ATMP:PESA = 2:1 by mass) and P_5E (PESA:EDTMPS = 5:1 by mass) were selected to probe the possible anti-scaling mechanism. The $CaSO_4{\cdot}2H_2O$ scales deposited were analyzed by X-ray diffraction and scanning electron microscopy, then the results manifested that the combination of PESA with ATMP or EDTMPS markedly reduced the particle size of the scales and thus synergistically inhibited the formation of $CaSO_4{\cdot}2H_2O$ scales.

Keywords: Scale inhibitor; ATMP; PESA; EDTMPS; Synergistic effect

1. Introduction

Water injection is an efficient way to enhance the recovery ratio of crude oil by supplementing reservoir energy and maintaining strata pressure [1–3]. In general, three types of water sources are used in oilfields: clean water, oily wastewater, and seawater [4–6]. Clean water [7,8] is usually used in the early stage of petroleum production, and oily wastewater [9–11] is mainly used in the middle and late stages of petroleum production. As the clean water and oily wastewater are injected into the stratum and mixed with the previously strata water, the anions in the injected water such as SO_4^{2-} and CO_3^{2-} will react with the cations like Ca^{2+} and Ba^{2+} in the strata water to generate scales. The scales mainly include $CaCO_3$ scales [12–16], $CaSO_4{\cdot}2H_2O$ scales [17–21] and $BaSO_4$ scales [22,23], which will block pipes and equipment, then result in a huge economic loss [24]. At the same time, the balance in original strata water will be destroyed due to the changes caused by temperature [25,26], pressure [27] and pH value in the process of water injection. Then, the formation of scales will be further aggravated. These scales will lead to serious problems for the production and development of petroleum in oilfields.

It was believed that the formation of scale deposits consists of two continuous processes: the diffusion and migration of ions towards the crystalline surface and the growth of the crystal particles [28]. The methods to control the formation of scales mainly include removing some scale-forming ions such as Ca^{2+}, Ba^{2+}, CO_3^{2-}, and SO_4^{2-} [29] and introducing acid or gaseous carbon dioxide into the solution [30]. At the same time, reducing the pH value of the solution and stabilizing the bicarbonate also facilitate

* Corresponding author.

the inhibition of scales. This work is intended to inhibit the formation of scales by antiscalants in the process of petroleum production, especially when a lot of Ca^{2+}, Ba^{2+}, CO_3^{2-}, and SO_4^{2-} ions are present in the reinjected wastewater.

Inhibitors are often adsorbed on different crystal surfaces selectively, including kink sites, steps, ledges, and faces [31]. The scale-inhibiting role of chemical reagent was supposed to proceed by solubilization, lattice distortion, condensation and dispersion, regeneration-self-releasing membrane hypothesis or double electric layer mechanism.

Individual antiscalants were well investigated by researchers [32–36]. Liu et al. [32] compared the anti-scaling performance of polyepoxysuccinic acid (PESA) to polyaspartic acid (PASP) against the formation of $CaSO_4{\cdot}2H_2O$, $CaCO_3$, $SrSO_4$ and $BaSO_4$ scales in the cooling water system. It was found that PESA possessed better scale-inhibiting capability than PASP for $CaCO_3$ and $SrSO_4$ scales, while PASP exhibited a more excellent anti-scaling role on the formation of $CaSO_4{\cdot}2H_2O$ and $BaSO_4$ scales. Popov et al. [33] probed the scale inhibiting performance of four phosphorous-free polymers and three phosphonates for $CaSO_4{\cdot}2H_2O$ scales, and found a sequence of the scale-inhibiting capability of seven kinds of scale inhibitors: copolymer of maleic and acrylic acid (MA-AA) ~ amino trimethylene phosphonic acid (ATMP) > PESA (400–1,500 Da) > PASP (1,000–5,000 Da) >> polyacrylic acid sodium salt (PAAS) (3,000–5,000 Da) ~ 2-phosphonobutane-1,2,4-tricarboxylic acid (PBTC) ~ 1-hydroxyethane-1,1-bis (phosphonic acid) (HEDP). Zeino et al. [34] studied the anti-scaling performance of five kinds of scale inhibitors under the three different elevated saturation indexes for calcium sulfate scale and found that the combined inhibitors of ATMP with diethylenetriamine penta(methylene phosphonic acid) (DTPMPA) presented the highest scale-inhibiting rate and longest induction times at a relatively low concentration. Han et al. [35] investigated the effect of ethylene diamine tetra (methylene phosphonic acid) sodium (EDTMPS) on calcium carbonate precipitation under alternating electromagnetic field and ultrasonic treatment, and a scale inhibition efficiency of 71.16% was observed when the EDTMPS was applied at a dosage of 7.5 mg L^{-1}. In addition, a soluble, highly efficient and versatile scale inhibitor (PESA) was prepared by Zhou et al. [36].

However, individual antiscalants are often found limited scale-inhibiting capability or needed a relatively high concentration to realize a desired anti-scaling effect, and thus researchers had tried the possibility of the combination of two or more scale inhibitors. Some researches [37,38] probed the synergistic effects between phosphonates and polymers on inhibiting calcium carbonate scales in the cooling water system. Shaw et al. [39] observed a synergy between phosphonate and polymeric antiscalants for inhibiting the formation of barium sulfate scales. Ou et al. [40] investigated the synergistic effect of sodium gluconate (SG) and PBTC against the formation of $CaCO_3$ scale in an open cooling water system. The experimental results showed that SG slowed down the germination rate of $CaCO_3$ by 4.3 times compared with the individual PBTC, which could be expected to replace phosphonate scale inhibitors.

Phosphonates and polymers have different function mechanism on scale inhibition, and their blends are hoped to enhance anti-scaling performance than individual inhibitors. To the best of our knowledge, there was no report about the blended antiscalants of PESA and EDTMPS or ATMP. Furthermore, PESA is environmentally more friendly than phosphonate scale inhibitors, and the combination of phosphonate with PESA might reduce the amount of phosphonate and thus become environmentally acceptable. This work is designed to investigate the synergistic role of every two-scale inhibitors among ATMP, PESA, and EDTMPS by a static scale-inhibiting test based on $CaSO_4{\cdot}2H_2O$ scales. The synergistic mass rate between inhibitors was determined, and the possible scale inhibition mechanism was probed.

2. Experimental section

2.1. Reagents

ATMP, $N(CH_2PO_3H_2)_3$, molecular mass: 299.05 Da, (PESA, $HO(C_4H_2O_5M_2)_nH$, molecular mass: 400–1,500 Da) and (EDTMPS, $C_6H_{12}O_{12}N_2P_4Na_8$, molecular mass: 612.13 Da) was purchased from Shandong Taihe Water Treatment Technologies Co. Ltd. Calcium chloride and sodium sulfate were purchased from Sinopharm. ("Sinopharm" is a Water Treatment Agent located at Industrial Park, Shizhong District, Zaozhuang City, Shandong Province (Shiliquan East Road 1#)). All reagents were used without pretreatment.

2.2. Method for static scale inhibition

The scale inhibition rate for $CaSO_4{\cdot}2H_2O$ was tested by the complexometric titration of ethylene diamine tetraacetic acid (EDTA). 180 mL of deionized water and 25 mL of $CaCl_2$ solution (83.25 g L^{-1}) were introduced into a 250 mL of volumetric flask followed by a periodic shaking. The calculated amount of scale inhibitors and 25 mL of Na_2SO_4 solution (108.5 g L^{-1}) were added into the above $CaCl_2$ solution in sequence, then diluted up to 250 mL by deionized water. The resulted supersaturation index was ca. 2.4. A pH value of ca. 5 was observed after enough shaking. The resulting solution was placed in a stoppered flask of 250 mL and was kept at 50°C ± 1°C for 24 h in a water bath. The experiments were also performed in the absence of either scale inhibitors or both Na_2SO_4 solution and scale inhibitors as blank tests. The concentration of calcium ions that were not combined with SO_4^{2-} anions were analyzed by complexometric titration of EDTA to determine the scale-inhibiting rate. All operations were rigorously carried out according to the standard Q/SY 126-2007 (corrosion and scale inhibitor for oilfield produced water treatment). In addition, the possible reactions between the calcium ions and inhibitors (ATMP, PESA, and EDTMPS) were investigated using the same method as the inhibition rate of the $CaSO_4{\cdot}2H_2O$ scale except for an absence of SO_4^{2-}.

2.3. Characterization of $CaSO_4{\cdot}2H_2O$ scales

The crystal morphologies of the $CaSO_4{\cdot}2H_2O$ scales which was generated by adding a different concentration of scale inhibitors were observed by an S-4800 field emission scanning electron microscopy (SEM). X-ray diffraction (XRD) spectra were obtained by a Bruker D8 Advance X-ray diffractometer (Beijing Bruckstr. 16, saarbrücken). The 2θ degree scans covered a range of 10°–60°, and the applied voltage and electric current were 25 kV and 25 mA, respectively.

3. Results and discussion

3.1. Investigation on the reaction between Ca^{2+} and antiscalants

The possible reactions between Ca^{2+} and inhibitors were investigated by adding ATMP, PESA, EDTMPS or their combinations to the aqueous solution of calcium chloride, and the results are summarized in Table 1. There was a decrease of Ca^{2+} concentration less than 0.60% observed on the resulting solutions, which was much lower than the error range. This indicated that the reactions between calcium ions and inhibitors are negligible under the applied test conditions.

3.2. Anti-scaling performance of individual antiscalants

The scale-inhibiting performance of individual inhibitors for $CaSO_4{\cdot}2H_2O$ scale was determined by complexometric titration of EDTA with a concentration of inhibitors ranging from 5 to 30 mg L^{-1} and a step of 5 mg L^{-1}, and the results are shown in Fig. 1. It was found that EDTMPS exhibited an excellent scale-inhibiting capability for $CaSO_4{\cdot}2H_2O$ scale with an anti-scaling rate up to 93.3% when 10 mg L^{-1} of EDTMPS was used. However, the scale-inhibiting performance was not improved significantly when the concentration of EDTMPS was increased further, indicating that EDTMPS possesses a significant threshold effect on the anti-scaling performance for the $CaSO_4{\cdot}2H_2O$ scale. This phenomenon can be attributed to the adsorption characteristics of EDTMPS on the surface of $CaSO_4{\cdot}2H_2O$ scales. These scale inhibitors would be adsorbed on the surface of the specific crystal to inhibit the further growth of crystals, and presented a characteristic of Langmuir monolayer adsorption. Therefore, the scale-inhibiting rate increased with the enhancement of the concentration of the scale inhibitor until the threshold was reached.

The scale-inhibiting performances of ATMP and PESA for $CaSO_4{\cdot}2H_2O$ scales were much lower than that of EDTMPS. The anti-scaling rate increased with an increasing concentration of the scale inhibitors. ATMP presented better scale-inhibiting capability than PESA when the concentration of scale inhibitors were less than 10 mg L^{-1}, which was consistent with the result obtained by Popov et al. [33]. However, PESA exhibited a stronger capability against the formation of the $CaSO_4{\cdot}2H_2O$ scale than ATMP when their concentrations were more than 10 mg L^{-1}. The scale-inhibiting rates of both ATMP and PESA were found a continuous rise when their concentrations were increased, suggesting that satisfactory performance can be reached at a relatively high concentration of ATMP or PESA. However, it was reported that ATMP possessed a high scale-inhibiting rate at a lower concentration. The scale-inhibiting experiments reported were carried out at room temperature with a supersaturation index of 2.5 in comparison with ours performed at 50°C with a similar supersaturation index (2.4). The increase in temperature has a limited influence on the solubility of $CaSO_4{\cdot}2H_2O$ scales [41]. However, the brine containing 0.1 mol L^{-1} of NaCl was adopted in the reference, which was unfavorable for the formation of $CaSO_4{\cdot}2H_2O$ scales because of the solubilization role of NaCl [42]. No NaCl or other salts were used in this work, leading to a higher concentration of ATMP.

3.3. Synergistic effect between ATMP and PESA for the inhibition of $CaSO_4{\cdot}2H_2O$ scale

Fig. 2 shows the scale-inhibiting performances of the blend inhibitors of ATMP and PESA for $CaSO_4{\cdot}2H_2O$ scales, and the total concentration of the blend inhibitors added was kept constant (30 mg L^{-1}) in the experiment. It can be seen that the scale-inhibiting performance of the blend scale inhibitors for $CaSO_4{\cdot}2H_2O$ scales was markedly higher than that of the individual ATMP or PESA inhibitor under the same condition. The scale-inhibiting rate can reach more than 90% no matter what ratio of ATMP/PESA was applied, indicating that there was an excellent synergistic effect between ATMP and PESA for the inhibition of $CaSO_4{\cdot}2H_2O$ scales. It was believed that ATMP can block better one sort of "nanodust" particles, while PESA is capable of blocking better another sort during the induction time [43–45]. Accordingly, a mixture of ATMP and PESA might become more efficient than the individual, and the ($-PO(OH)_2$) group in ATMP and the (–COOH) group in PESA cooperated reinforced the inhibition effect.

3.4. Synergistic effect between ATMP and EDTMPS for the inhibition of $CaSO_4{\cdot}2H_2O$ scale

Fig. 3 shows the scale-inhibiting performance of the blend inhibitors of ATMP & EDTMPS for $CaSO_4{\cdot}2H_2O$ scales, and the concentration of the blend inhibitors added was kept at 30 mg L^{-1} in this experiment. It can be seen that the anti-scaling rate of the blend scale inhibitors increased with the enhancement of the relative concentration of EDTMPS.

Table 1
The Ca^{2+} concentration with inhibitors but without sulfate ions

Inhibitors	Initial concentration (Ca^{2+}), mol L^{-1}	Final concentration (Ca^{2+}), mol L^{-1}	Change rate, %
ATMP	0.0750	0.0748	0.27
PESA	0.0750[1]	0.0750	0.00
EDTMPS	0.0750	0.0748	0.27
ATMP + PESA	0.0750	0.0750	0.00
ATMP + EDTMPS	0.0750	0.0746	0.53
PESA + EDTMPS	0.0750	0.0748	0.27

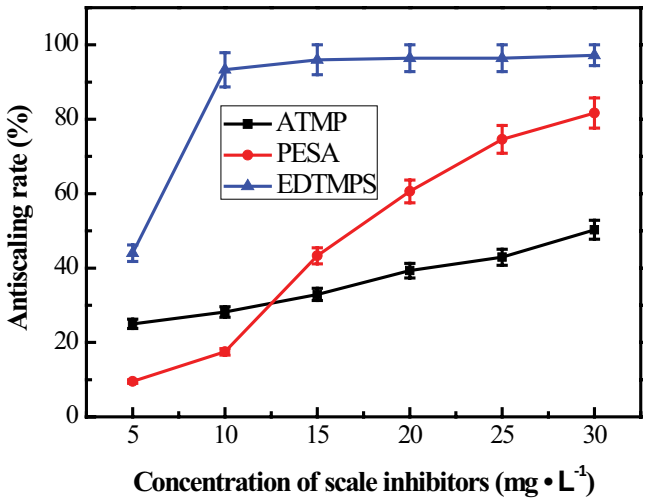

Fig. 1. Scale-inhibiting performances of individual scale inhibitors for $CaSO_4 \cdot 2H_2O$ scales.

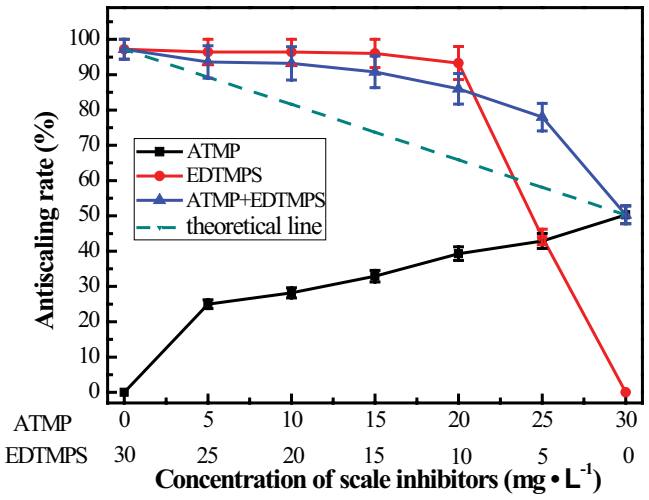

Fig. 3. Scale-inhibiting performances of the blend inhibitors of ATMP and EDTMPS for $CaSO_4 \cdot 2H_2O$ scales.

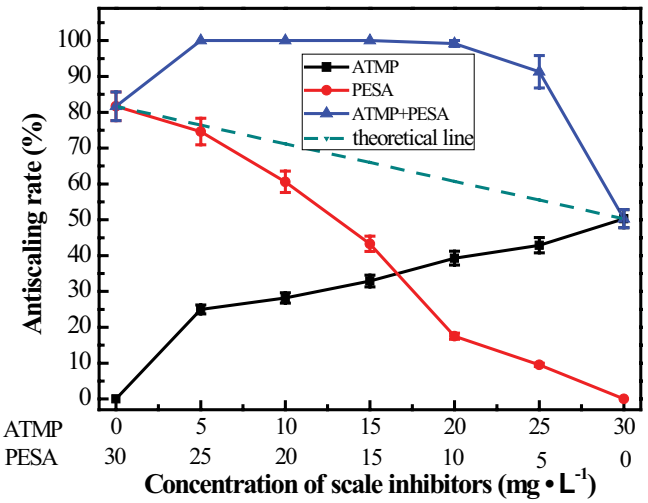

Fig. 2. Scale-inhibiting performances of the blend inhibitors of ATMP and PESA for $CaSO_4 \cdot 2H_2O$ scales.

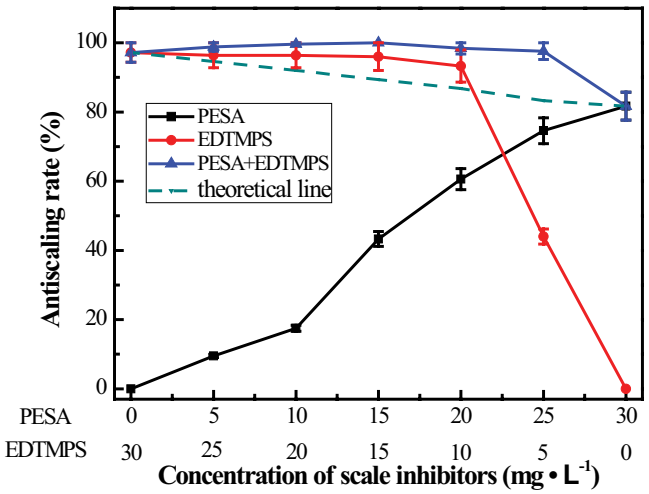

Fig. 4. Scale-inhibiting performance of the blend inhibitors of PESA and EDTMPS for $CaSO_4 \cdot 2H_2O$ scales.

However, the scale-inhibiting performances of the blends were lower than that of the individual antiscalant of EDTMPS for $CaSO_4 \cdot 2H_2O$ scales but higher than that of ATMP. Both ATMP and EDTMPS belong to organic phosphonic scale inhibitors with a similar scale inhibition mechanism, and EDTMPS exhibited more efficient scale-inhibiting capability than ATMP (Fig. 1). Therefore, there was no apparent synergistic effect observed between ATMP and EDTMPS and the blends showed a lower scale-inhibiting rate than EDTMPS.

3.5. Synergistic effect between PESA and EDTMPS for the inhibition of $CaSO_4 \cdot 2H_2O$ scales

Fig. 4 shows the scale-inhibiting performance of the blend inhibitors of PESA and EDTMPS for $CaSO_4 \cdot 2H_2O$ scales, in which the concentration of the blends was kept at 30 mg L^{-1}. It can be seen that the scale-inhibiting rates of the blends on the $CaSO_4 \cdot 2H_2O$ scales were first stable and then slightly decreased with the increase of the relative concentration of PESA, but they were higher than that of the individual inhibitor under the same conditions, indicating that there was an obvious synergistic effect between PESA and EDTMPS. Especially, a remarkable synergy was observed when the dosages of PESA and EDTMPS were 25 and 5 mg L^{-1}, respectively. In consideration of the fact that EDTMPS and PESA belong to different types of scale inhibitors, it was supposed that EDTMPS and PESA can block different sorts of "nanodust" particles. Thus, a combination of EDTMPS with PESA became more efficient than the individual antiscalant [43]. Furthermore, the $(-PO(OH)_2)$ in EDTMPS as a strong acid group can promote solubilization of the scale, while the (–COOH) groups in PESA, which show weaker acidity than the $(-PO(OH)_2)$ groups, can be adsorbed on the surface of the crystals to prevent the growth of $CaSO_4 \cdot 2H_2O$ scales.

3.6. XRD analysis of $CaSO_4$ scale

XRD was used to study the scale-inhibiting mechanism of the blend scale inhibitors for the $CaSO_4·2H_2O$ scale by tuning the kinds of scale inhibitors, and the results are shown in Fig. 5. It can be seen that the crystal deposited in the solution were $CaSO_4·2H_2O$ crystals when there was no scale inhibitor added. Its XRD pattern presented the strong characteristic diffraction peaks, indicating that the resulting $CaSO_4·2H_2O$ scales possessed a big crystal size and a high crystallinity in the absence of inhibitors. The intensity of diffraction peaks of the $CaSO_4·2H_2O$ scale were found a decrease in a sequence of ATMP > PESA > EDTMPS > P_5E > A_2P when the scale inhibitors were added. It was found that the $CaSO_4·2H_2O$ scales from the blends exhibited smaller crystal sizes than those from the individual inhibitors, which was in line with the scale-inhibiting capability of the inhibitors (Figs. 2–4). The weakest XRD peaks were observed on the scales from A_2P (Fig. 5e), indicating that the blends possessed the strongest scale-inhibiting capability among the investigated ones.

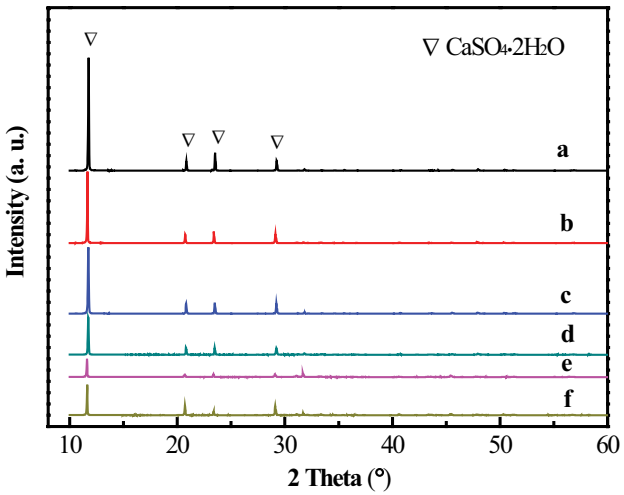

Fig. 5. XRD patterns of $CaSO_4·2H_2O$ scales (a) without inhibitor and with the inhibitors of (b) 30 mg L^{-1} ATMP, (c) 30 mg L^{-1} PESA, (d) 30 mg L^{-1} EDTMPS, (e) 30 mg L^{-1} A_2P, and (f) 30 mg L^{-1} P_5E.

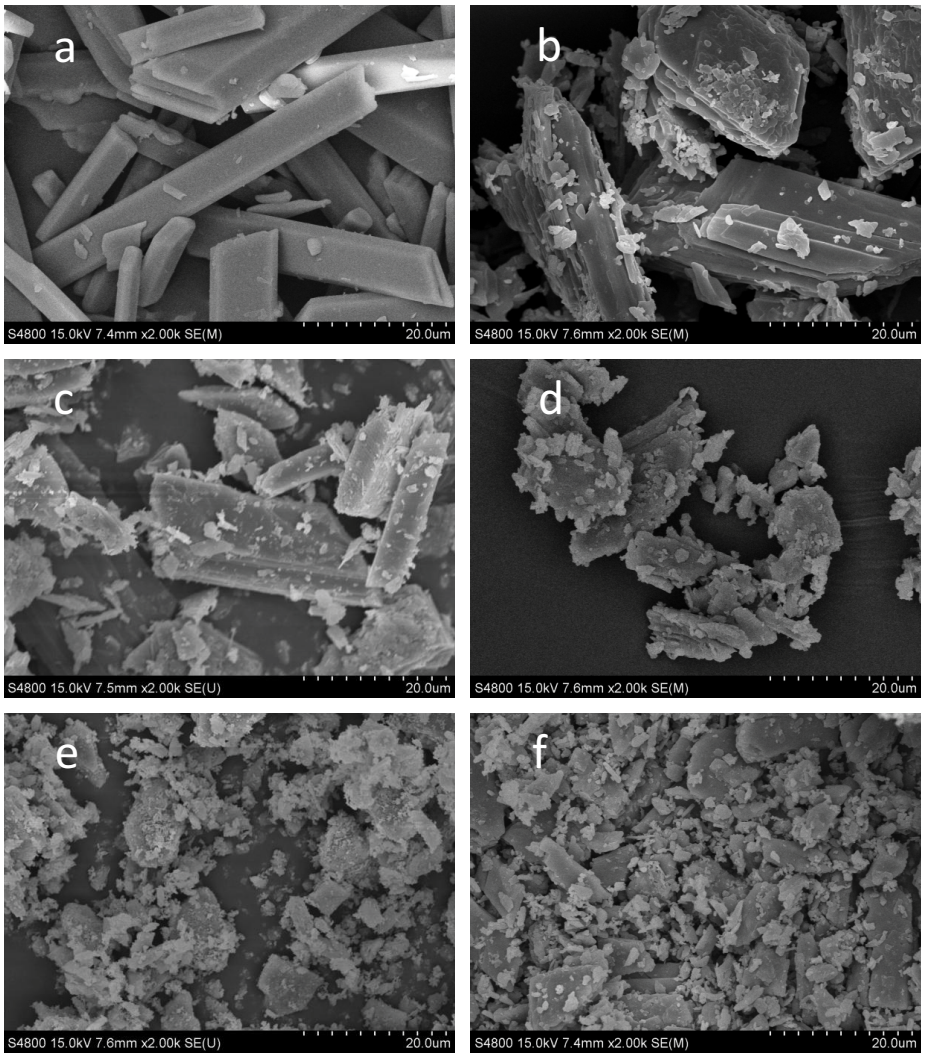

Fig. 6. Scanning electron microscopy images of $CaSO_4·2H_2O$ scales (a) without inhibitors and with inhibitors (b) 30 mg L^{-1} ATMP, (c) 30 mg L^{-1} PESA, (d) 30 mg L^{-1} EDTMPS, (e) 30 mg L^{-1} A_2P, and (f) 30 mg L^{-1} P_5E.

3.7. SEM analysis of the $CaSO_4 \cdot 2H_2O$ scales

To probe the scale inhibition mechanism more intuitively, the SEM images were taken to observe the morphologies of $CaSO_4 \cdot 2H_2O$ scales generated by adding different scale inhibitors, and the results are shown in Fig. 6. It can be seen that the $CaSO_4 \cdot 2H_2O$ scales presented a rod-like shape with a regular configuration and smooth surface when there was no scale inhibitor added, which was a crystal of dihydrate calcium sulfate. Tentatively, the formation of gypsum crystals was carried out by a heterogeneous nucleation mechanism in the blank experiment: the gypsum phase was formed on the surface of the impurities. The anti-scaling molecules did not block the gypsum tiny crystals but the "nanodust" particles and the scale formation were inhibited. The rod crystals were distorted obviously upon addition of scale inhibitors, and the surface of $CaSO_4 \cdot 2H_2O$ scale became coarser and the particle size of the scale was observed a sharp decrease. This can be ascribed to the decrease of the crystallinity of the $CaSO_4 \cdot 2H_2O$ scale, which well agreed with the results observed in their XRD patterns in Fig. 5. The looser structure of $CaSO_4 \cdot 2H_2O$ scales might prevent the growth of the scales and thus significantly enhance the scale-inhibiting rate. It was observed that the size of $CaSO_4 \cdot 2H_2O$ scales decreased in the sequence of ATMP > blank > PESA > EDTMPS > P_5E > A_2P, roughly in line with their scale inhibition rates.

It is worthwhile to note that the $CaSO_4 \cdot 2H_2O$ scales obtained in the presence of antiscalants presented larger particle size than that from the blank test in spite of its high scale inhibition rate. The similar results were observed by other researchers [43]. Among all individual scale inhibitors, EDTMPS exhibited the best anti-scaling performance, and ATMP presented the worst scale-inhibiting capability. Further, the scale-inhibiting performance of the blend scale inhibitors were better than that of single scale inhibitor, and A_2P had the best scale inhibition performance under the experimental conditions adopted in this work.

4. Conclusions

EDTMPS exhibited the best scale-inhibiting capability for $CaSO_4 \cdot 2H_2O$ scales among the investigated individual ATMP, PESA and EDTMPS inhibitors under the same experimental conditions. A remarkable synergistic effect was observed between ATMP and PESA in an arbitrary proportion against the formation of gypsum, and PESA and EDTMPS also showed a marked synergistic effect in a PESA/EDTMPS mass ratio of 5:1. However, there was no synergistic effect between ATMP and EDTMPS. Supposedly, phosphonate inhibitors can block better one kind of "nanodust" particles, while PESA can do better another kind, and thus the combination of ATMP/EDTMPS and PESA might be more effective than the individual inhibitor.

Acknowledgment

The authors gratefully acknowledge a project funded by the Priority Academic Program Development of Jiangsu Higher Education Institutions.

References

[1] X.Y. Liu, J.G. Li, Q.Y. Zhu, J.L. Feng, Y.L. Li, J.X. Sun, The analysis and prediction of scale accumulation for water-injection pipelines in the Daqing Oilfield, J. Pet. Sci. Eng., 66 (2009) 161–164.
[2] G.L. Jing, S. Tang, X.X. Li, H.Y. Wang, The analysis of scaling mechanism for water-injection pipe columns in the Daqing Oilfield, Arabian J. Chem., 10 (2017) S1235–S1239.
[3] Z.W. Yuan, B.Q. Yang, L. Yang, W.H. Gu, X. Chen, B.T. Kang, C.X. Li, H.L. Zhang, Water-cut rising mechanism and optimized water injection technology for deepwater turbidite sandstone oilfield: a case study of AKPO oilfield in Niger Delta Basin, West Africa, Pet. Explor. Dev., 45 (2018) 302–311.
[4] B.W. Su, M.W. Dou, X.L. Gao, Y.W. Shang, C.J. Gao, Study on seawater nanofiltration softening technology for offshore oilfield water and polymer flooding, Desalination, 297 (2012) 30–37.
[5] M.S.H. Bader, Seawater versus produced water in oil-fields water injection operations, Desalination, 208 (2007) 159–168.
[6] W. van Berk, Y.J. Fu, H.M. Schulz, Temporal and spatial development of scaling in reservoir aquifers triggered by seawater injection: three-dimensional reactive mass transport modeling of water–rock–gas interactions, J. Pet. Sci. Eng., 135 (2015) 206–217.
[7] M. Salman, H. Qabazard, M. Moshfeghian, Water scaling case studies in a Kuwaiti oil field, J. Pet. Sci. Eng., 55 (2007) 48–55.
[8] H.B. Ghalib, I.A.R. Almallah, Scaling simulation resulting from mixing predicted model between Mishrif formation water and different waters injection in Basrah oil field, southern Iraq, Model. Earth Syst. Environ., 3 (2017) 1557–1569.
[9] M. Melo, H. Schluter, J. Ferreira, R. Magda, A. Júnior, O. de Aquino, Advanced performance evaluation of a reverse osmosis treatment for oilfield produced water aiming reuse, Desalination, 250 (2010) 1016–1018.
[10] B. Dong, Y. Xu, H. Deng, F. Luo, S.J. Jiang, Effects of pipeline corrosion on the injection water quality of low permeability in oilfield, Desalination, 326 (2013) 141–147.
[11] A. Fakhru'l-Razi, A.R. Pendashteh, Z.Z. Abidin, L.C. Abdullah, D.R.A. Biak, S.S. Madaeni, Application of membrane-coupled sequencing batch reactor for oilfield produced water recycle and beneficial re-use, Bioresour. Technol., 101 (2010) 6942–6949.
[12] M.-A. Ahmadi, A.R. Bahadori, S.R. Shadizadeh, A rigorous model to predict the amount of dissolved calcium carbonate concentration throughout oil field brines: side effect of pressure and temperature, Fuel, 139 (2015) 154–159.
[13] X.X. Yang, W. Li, L.J. Guo, X.J. Liu, H.Q. Feng, Prediction of $CaCO_3$ scaling in water injection wellbore, Appl. Therm. Eng., 98 (2016) 532–540.
[14] A. Khormali, D.G. Petrakov, M.J.A. Moein, Experimental analysis of calcium carbonate scale formation and inhibition in waterflooding of carbonate reservoirs, J. Pet. Sci. Eng., 147 (2016) 843–850.
[15] M. El-Said, M. Ramzi, T. Abdel-Moghny, Analysis of oilfield waters by ion chromatography to determine the composition of scale deposition, Desalination, 249 (2009) 748–756.
[16] A. Kamari, F. Gharagheizi, A. Bahadori, A.H. Mohammadi, Determination of the equilibrated calcium carbonate (calcite) scaling in aqueous phase using a reliable approach, J. Taiwan Inst. Chem. Eng., 45 (2014) 1307–1313.
[17] Y.Z. Zhao, L.L. Jia, K.Y. Liu, P. Gao, H.H. Ge, L.J. Fu, Inhibition of calcium sulfate scale by poly (citric acid), Desalination, 392 (2016) 1–7.
[18] I. Atamanenko, A. Kryvoruchko, L. Yurlova, E. Tsapiuk, Study of the $CaSO_4$ deposits in the presence of scale inhibitors, Desalination, 147 (2002) 257–262.
[19] Q. Zhao, Y. Liu, S. Wang, Surface modification of water treatment equipment for reducing $CaSO_4$ scale formation, Desalination, 180 (2005) 133–138.
[20] Y.W. Choi, G. Naidu, S.Y. Jeong, S.H. Lee, S. Vigneswaran, Effect of chemical and physical factors on the crystallization of calcium sulfate in seawater reverse osmosis brine, Desalination, 426 (2018) 78–87.

[21] A. Quddus, L.M. Al-Hadhrami, Hydrodynamically deposited CaCO3 and CaSO4 scales, Desalination, 246 (2009) 526–533.
[22] A.B. BinMerdhah, Inhibition of barium sulfate scale at high-barium formation water, J. Pet. Sci. Eng., 90–91 (2012) 124–130.
[23] K. Peyvandi, A. Haghtalab, M.R. Omidkhah, Using an electrochemical technique to study the effective variables on morphology and deposition of $CaCO_3$ and $BaSO_4$ at the metal surface, J. Cryst. Growth, 354 (2012) 109–118.
[24] J.B. Li, M.J. Tang, Z.R. Ye, L.L. Chen, Y.Q. Zhou, Scale formation and control in oil and gas fields: a review, J. Dispersion Sci. Technol., 38 (2017) 661–670.
[25] S.J. Dyer, G.M. Graham, The effect of temperature and pressure on oilfield scale formation, J. Pet. Sci. Eng., 35 (2002) 95–107.
[26] S. Mohammadi, F. Rashidi, S.A. Mousavi-Dehghani, M.-H. Ghazanfari, Modeling of asphaltene aggregation phenomena in live oil systems at high pressure-high temperature, Fluid Phase Equilib., 423 (2016) 55–73.
[27] M. Mahmoud, S. Elkatatny, K.Z. Abdelgawad, Using high- and low-salinity seawater injection to maintain the oil reservoir pressure without damage, J. Pet. Explor. Prod. Technol., 7 (2017) 589–596.
[28] X.H. Li, H. Shemer, D. Hasson, R. Semiat, Characterization of the effectiveness of anti-scalants in suppressing scale deposition on a heated surface, Desalination, 397 (2016) 38–42.
[29] T. Gu, P.C. Su, X.Y. Liu, J.C. Zou, X.Y. Zhang, Y. Hu, A composite inhibitor used in oilfield: MA-AMPS and imidazoline, J. Pet. Sci. Eng., 102 (2013) 41–46.
[30] Q.L. Wu, Z.H. Zhang, X.M. Dong, J.Q. Yang, Corrosion behavior of low-alloy steel containing 1% chromium in CO_2 environments, Corros. Sci., 75 (2013) 400–408.
[31] T.A. Hoang, Mechanisms of Scale Formation and Inhibition, Z. Amjad, K. Demadis, Eds., Mineral Scales and Deposits, Scientific and Technological Approaches, 1st ed., Elsevier, 2015, pp. 47–83.
[32] D. Liu, W.B. Dong, F.T. Li, F. Hui, J. Lédion, Comparative performance of polyepoxysuccinic acid and polyaspartic acid on scaling inhibition by static and rapid controlled precipitation methods, Desalination, 304 (2012) 1–10.
[33] K. Popov, G. Rudakova, V. Larchenko, M. Tusheva, S. Kamagurov, J. Dikareva, N. Kovaleva, A comparative performance evaluation of some novel "green" and traditional antiscalants in calcium sulfate scaling, Adv. Mater. Sci. Eng., 2016 (2016) 10 p, http://dx.doi.org/10.1155/2016/7635329.
[34] A. Zeino, M. Albakri, M. Khaled, M. Zarzour, Comparative study of the synergistic effect of ATMP and DTPMPA on $CaSO_4$ scale inhibition and evaluation of induction time effect, J. Water Process Eng., 21 (2018) 1–8.
[35] Y. Han, C.X. Zhang, L. Zhu, Q.F. Gao, L.C. Wu, Q.R. Zhang, R.K. Zhao, Effect of alternating electromagnetic field and ultrasonic on $CaCO_3$ scale inhibitive performance of EDTMPS, J. Taiwan Inst. Chem. Eng., 99 (2019) 104–112.
[36] X.H. Zhou, Y.H. Sun, Y.Z. Wang, Inhibition and dispersion of polyepoxysuccinate as a scale inhibitor, J. Environ. Sci., 23 (2011) S159–S161.
[37] Z. Amjad, Part 3: performance of polymers, phosphonates, and polymer/phosphonate blends as gypsum scale inhibitors, Ultrapure Water, 27 (2010) 30–35.
[38] K.D. Demadis, S.D. Katarachia, Metal-phosphonate chemistry: synthesis, crystal structure of calcium-amino-*tris*-(methylene phosphonate) and inhibition of $CaCO_3$ crystal growth, Phosphorus Sulfur Rel. Elem., 179 (2004) 627–648.
[39] S.S. Shaw, K.S. Sorbie, Synergistic properties of phosphonate and polymeric scale inhibitor blends for barium sulfate scale inhibition, SPE Prod. Oper., 30 (2015) 16–25.
[40] H.-H. Ou, L.-H. Chiang Hsieh, A synergistic effect of sodium gluconate and 2-phosphonobutane-1,2,4-tricarboxylic acid on the inhibition of $CaCO_3$ scaling formation, Powder Technol., 302 (2016) 160–167.
[41] Q.X. Chen, L.C. Yang, M. Chen, J.F. Zhang, Y. Huang, Study of the influence factors of calcium sulfate dihydrate crystallization, Nat. Sci. J. Xiangtan Univ., 36 (2014) 60–66.
[42] Z.L. Cao, J.F. Chen, Y. Liu, P.K. Luo, Y. Zhang, C.X. Lu, The solubility of scale forming minerals $CaSO_4{\cdot}2H_2O$ and $CaCO_3$ in oilfield produced water, Chem. Eng. Oil Gas, 35 (2006) 473–477.
[43] K.I. Popov, M.S. Oshchepkov, E. Afanas'eva, E. Koltinova, Y. Dikareva, H. Rönkkömäki, A new insight into the mechanism of the scale inhibition: DLS study of gypsum nucleation in presence of phosphonates using nanosilver dispersion as an internal light scattering intensity reference, Colloids Surf., A, 560 (2019) 122–129.
[44] K.I. Popov, M.S. Oshchepkov, N.A. Shabanova, Y.M. Dikareva, V.E. Larchenko, E.Y. Koltinova, DLS study of a phosphonate induced gypsum scale inhibition mechanism using indifferent nanodispersions as the standards of a light scattering intensity comparison, Int. J. Corros. Scale Inhib., 7 (2018) 9–24.
[45] M. Oshchepkov, S. Kamagurov, S. Tkachenko, A. Ryabova, K. Popov, Insight into the mechanisms of scale inhibition: a case study of a task-specific fluorescent-tagged scale inhibitor location on gypsum crystals. ChemNanoMat, 5 (2019) 586–592.